Study on the integration characteristics of an integrated solar combined cycle system

Liqiang Duan[a], Wanjun Qu[b], Long Yue[c], Shilun Jia[d] and Yongping Yang[e]

[a]North China Electric Power University, Beijing, China, dlq@ncepu.edu.cn
[b]North China Electric Power University, Beijing, China, 867836926@qq.com
[c]North China Electric Power University, Beijing, China, 542351917@qq.com
[d]North China Electric Power University, Beijing, China, 469000412@qq.com
[e]North China Electric Power University, Beijing, China, yyp@ncepu.edu.cn

Abstract:

On the base of the gas steam combined cycle system (GTCC) with the three-pressure reheat recovery steam generator (HRSG), the integrated trough solar energy combined cycle system (ISCC) is designed and optimized in limited collector aperture surface area. The Aspen Plus and TRNSYS software are applied in this paper to build the model of different systems. Results show that with the increase of design power, the annual solar thermal efficiency increases in the different integrations. When the two sections of HRSG simultaneously integrate with the solar system, its integrated power is the algebra of the power in each single-integration mode and the annual solar thermal efficiency is between the minimum and maximum efficiency of the single-integration modes. In the collector aperture area range of 5000m^2 to 287008m^2, this paper identifies the optimal integration schemes in which the solar energy is integrated with the single or double sections of HRSG. According to the quarterly characteristics of the single section integration, the reasonable quarterly integration can improve the system performance in the limited collector aperture area. For example when the design power is 30MW in the optimal integration mode of this paper, the annual efficiency of ISCC system is 13.2%, if the integrated positions are changed to LPB section in the first and fourth quarter, its annual efficiency is 14.29%, 1.09 percent points higher than the previous efficiency (13.2%), and 1.89 percent points higher than the highest efficiency (12.4%) of 30MW SEGS plants. So ISCC system has a significant thermodynamic advantage over an independent solar thermal power generation systems (SEGS), and is an effective solution to overcome the solar radiation fluctuation and some technology bottlenecks which include the immature heat storage technology. The achievements from this paper will provide the valuable guide for reforming GTCC to ISCC.

Keywords:

GTCC, Integrated power, Annual Solar Thermal Efficiency, The optimal integration schemes, ISCC.

1. Introduction:

Electric Power Research Institute [1] reported that, since 1985-1991, the California Mojave Desert has installed nine sets of trough solar thermal power generation systems with a total installed capacity of 354MW, and these systems are still in operation currently. The highest annual power generation efficiency of solar energy is 13.8%.

Under the background of the global environment pollution and energy issues in recent years, the solar energy thermal power generation has entered a new period of rapid development. In 2008,

German SM Company constructed the first 50MW solar energy thermal power generation plant in Spain and the second 50MW solar thermal power generation plant was put into operation in 2009. German SM Company has started to construct 250MW solar thermal power generation plant in Egypt. In China, the United States and other countries, a number of projects of trough concentrating solar thermal power have entered the early stage of the project work.

China National Renewable Energy Center [2] has proposed, in China, the solar thermal power generation will take the role of electricity supply of peaking load and intermediate load in 2020. After 2025-2030, it will provide the base load electricity supply and enter the electricity grid in parity. The period from 2015 to 2020 will be the main demonstration phase of the solar thermal power generation projects to accumulate experiences. The projects will begin to enter a large-scale development stage from 2020 to 2030.

References [3-5] summarize that the technology of the trough concentrating solar thermal power is currently the most mature commercial solar thermal power generation mode, at the same time, the solar thermal power tower technology faces with the problem of high cost and researches of the dish, solar chimneys and other solar thermal power technology are still at the experimental stage. However, the uneven geographical distributions of solar radiation, market policy and so on, to some extent, restrict the large-scale development of solar thermal power generation. The hybrid solar/fossil operation, with the advantage of reducing the technical and economic risks of using solar energy, is an effective solution to overcome the solar radiation fluctuation and some technology bottlenecks which include heat storage technology.

Integrated solar combined cycle (ISCC) system has become the focus of research in recent years. Giovanna Barigozzi [6] and G.Franchini [7] have studied the performance of tower and trough technology integrated with Brayton cycle and Rankine cycle, the results shows the integration of tower solar energy technology with Brayton cycle power has the maximum efficiency of transferring the solar energy to the electricity. A.Baghernejad, M.Yaghoubi [8-9] and GCBakos [10] have made some economic analysis of trough technology integrated with Rankine cycle, and explained the process of exergy loss and the relationship between the cost of electricity and integrations, that provided the valuable guide for technical improvements. M.J.Montes [11] and Antonio Rovira [12] compared the direct steam generation technology (DSG) with the traditional double-loop (HTF) technology. The results show DSG technology can effectively improve the performance of the integrated system. Guillermo Ordorica-Garcia [13] put forward a novel decarburization mode that includes separating CO_2 in the post-combustion of plants and reforming gasification of fossil fuel in pre-combustion of plants.

In this paper, on the base of an advanced gas steam combined cycle system that is consisted of GE PG9351FA gas turbine and a three-pressure reheat recovery steam generator (HRSG) and uses the Therminol VP-1 as heat transfer fluid (HTF), the trough solar system integrated with different sections of HRSG is studied to seek the optimal integration mode in the limited integration solar collector aperture area. At the same time, this paper analyzes the integration characteristics of different integrated sections in each quarter, which provides a deep understanding to make the most of solar energy.

2. System Description:

In this paper, the dual-loop integrated solar combined cycle system (ISCC) is composed of trough solar energy system and gas steam combined cycle system. Fig. 1 shows the detailed flow chart of ISCC system.

2.1. Gas turbine system process:

Air is compressed by the compressor of gas turbine, and a portion of the compressed air cools the turbine blades and other air combusts with the fuel (see Table 1) in the combustion chamber to generate the high temperature and high pressure flue gas which will expand in the turbine. Eventually the exhaust gas with the temperature of about 609℃ discharges into the HRSG.

Table 1. Natural gas fuel data

Composition	C1	C2	C3	IC4	NC4	IC5
Volume fraction (%)	96.23	1.77	0.30	0.062	0.075	0.02
Composition	NC5	C6	C7	CO2	N2	H2S
Volume fraction (%)	0.016	0.051	0.038	0.473	0.967	0.002

2.2. HRSG and steam turbine system process:

The feeding water is pressurized by the low pressure feed water pump and discharged into the low pressure economizer (LPE), the working medium is divided into three parts after the LPE, one part becomes the superheated steam through the low pressure evaporator (LPB) and the low pressure superheater (LPS), that mixes with the exhaust steam of the intermediate pressure cylinder (IT) and discharges into the low pressure cylinder (LT) to work, and the working medium flows into the condenser after expanding. The second part is pressurized by the intermediate pressure feed water pump and sequentially flows through the intermediate pressure economizer (IPE), the intermediate pressure evaporator (IPB), the intermediate pressure superheater (IPS), eventually mixes with the exhaust steam of the high pressure cylinder (HT) into the reheater (RH) and IT. The third part pressurized by the high pressure feed water pump sequentially flows through the first stage of the high pressure economizer (HPE1), the second stage high pressure economizer (HPE2), the high pressure evaporator (HPB), the high pressure superheater (HPS), and absorbs the flue gas heat to be the superheated steam flowing into the HT. During the process of system simulation, the temperature differences of both the pinch point and approach point are constant. The detailed operating parameters are shown in Table 4.

2.3. ISCC system process:

Fig. 1 shows a typical HPB section of combined cycle system integrates with the trough solar system to generate power. The working medium (water) from the HPE2 is divided into two parts, one part inflows the HPB, another part inflows the heat exchanger to absorb the heat energy of conduction oil to be the saturated vapor, finally these two parts medium mix into the HPS. In the process of heat transfer, the inlet and outlet temperatures of oil and water in heat exchanger are kept constant by adjusting the mass flow of water, when the solar radiation fluctuates over time. The integration methods of other heat transfer sections of combined cycle system are similar.

When two sections of HRSG simultaneously integrate with the solar energy to increase the power output, this paper uses two independent mirror arrays that have different integrated temperatures to maintain the minimum temperature difference (about 8℃) between the water and the conductive oil.

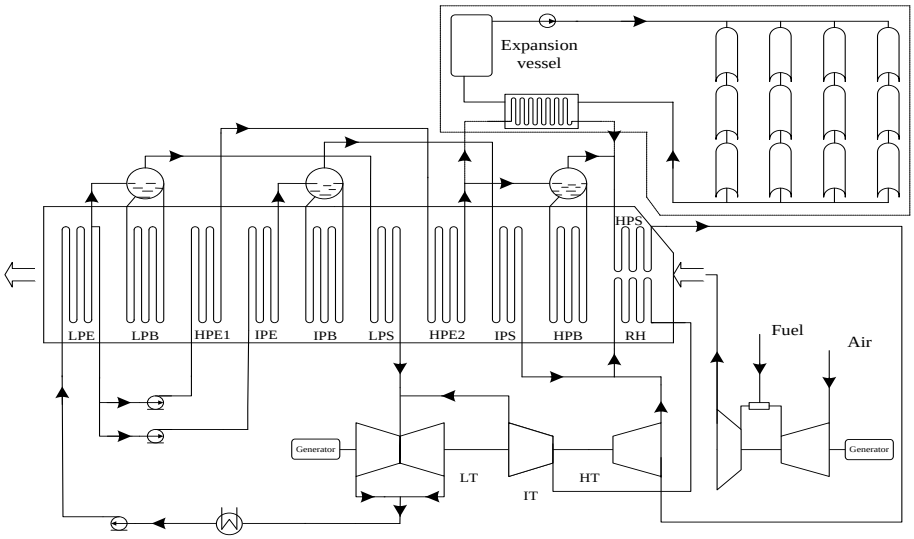

Fig. 1 Flow chart of ISCC system

3. Mathematical Model and Design Conditions

3.1. Gas turbine system model

In this paper, the Aspen Plus software is used to simulate the combined cycle system, in which the property methods of flue gas and working medium (water) are PR-BM and STEAM-TA respectively. In order to accurately build the model, this paper uses the air-cooled mathematical model of gas turbine proposed by Young and Wilcock [14-16]. The formula of the required cooling flow fraction φ is calculated with the following equation:

$$\varepsilon_0 = \left(T_{0g} - T_{met,ext}\right) \Big/ \left(T_{0g} - T_{0c,in}\right) \tag{1}$$

$$B = Bi_{tbc} - \left(\varepsilon_0 - \varepsilon_f\right) \Big/ \left(1-\varepsilon_0\right) \cdot Bi_{met} \tag{2}$$

$$\varphi = \frac{m_c}{m_g} = \frac{k_{cool}}{(1+B)} \left\{ \varepsilon_0 - \varepsilon_f \left[1 - \eta_{\text{int}} \left(1-\varepsilon_0\right) \right] \right\} \Big/ \left[\eta_{\text{int}} \left(1-\varepsilon_0\right) \right] \tag{3}$$

Where, T_{0g} is the relative total temperature of the mainstream gas; $T_{0c,in}$ is the relative total temperature of the coolant entering the blade passages; $T_{met,ext}$ is the allowable external surface metal temperature; Bi_{tbc} is the *TBC Biot number*; Bi_{met} is the *metal Biot number*; m_c and m_g are the flow rates of coolant and mainstream, respectively; K_{cool} is the *cooling flow factors*; ε_0 is the *blade cooling effectiveness*; ε_f is the *film cooling effectiveness*; η_{int} is the internal cooling efficiency. The detail parameters are shown in Table 2.

Table 2. Parameter values of cooling technology

Parameter	K_{cool}	η_{int}	ε_f	Bi_{tbc}	Bi_{met}	$T_{met,ext}$
Value	0.045	0.7	0.21	0.25	0.15	850℃

3.2. Gas turbine design conditions:

Table 3 lists the design data of gas turbine (GT). Table 4 lists the simulative results of system. It can be seen that the relative errors, to design values of the rated power, the rated thermal efficiency and

the exhaust temperature, are 0.47%, 0.38% and 0.02%, respectively. So this mathematical model of gas turbine is feasible.

Table 3. PG9351FA gas turbine design data

	Parameters	Values		Parameters	Values
Compressor	Inlet temperature	15℃	Turbine	Inlet temperature	1318℃
	Pressure ratio	15.4		Outlet temperature	609℃
	Inlet flow	623.7Kg/s	Gas turbine	Rated power	255.6MW
				Rated thermal efficiency	36.9%

Table 4. Design and simulation data of ISCC system

	Parameter	Value		Parameter	Value
Trough mirror	Width	1.52 m	Turbine(GT)	Mechanical efficiency	0.98
	Length	14.37m		Inlet temperature	1318℃
	Focal length	0.45 m		Exhaust temperature	609.1℃
	Row spacing	4.54 m	Stream Turbine	Isentropic efficiency(HP/IP/LP)	0.9/0.89/0.88
	Reflectivity	0.94	HRSG	Pinch temperature difference	12℃
	Cleanliness	0.95		Approach temperature difference	8℃
Collector	Internal diameter	55 mm		Exhaust temperature	86.18℃
Compressor(GT)	Pressure Loss	0.01		Steam pressure(HP/IP/LP)	16.5/3.5/0.4 MPa
	Pressure ratio	15.4		Steam temperature(HP/IP/LP)	565/350/265℃
	Isentropic efficiency	0.87	Brayton cycle	Output Power	256.81MW
	Mechanical efficiency	0.98		Thermal efficiency	37.04%
Combustor(GT)	Pressure Loss	0.03	Rankine cycle	Output Power	136.91MW
Turbine(GT)	Pressure Loss	0.01	Combined cycle	Output Power	393.72MW
	Isentropic efficiency	0.9		Thermal efficiency	56.78%

3.3. Trough solar system model:

This paper uses the TRNSYS to build the model of trough solar system, which requires more detailed parameters of trough solar system than other models. The thermal efficiency η of the cermet collector with annulus, which is proposed by Sandia National Laboratories to evaluate the test performance, is calculated with the following equation:

$$\eta = K \cdot M \cdot SH \cdot \left[A + B \cdot \frac{\Delta T_o + \Delta T_i}{2} \right] + \left(C + C_W \cdot W_S \right) \cdot \frac{\Delta T_o + \Delta T_i}{2 \cdot DNI} + D \cdot \frac{\Delta T_o \cdot \Delta T_i + \frac{1}{3}\left(\Delta T_o - \Delta T_i \right)^2}{DNI} \quad (4)$$

Where, K: the incident angle modifier; M: the end loss; SH: the collector shading; A, B, C, C_W, D: the loss coefficients; Ws: the wind speed; ΔT_0, ΔT_i: the temperature difference of HTF outlet and inlet temperature to ambient temperature; DNI: the direct solar radiation intensity.

The total heat losses of the trough solar system in pipe and expansion are calculated with the following empirical formula:

$$Q_{HeatLosses} = Q_{Piping} + Q_{ExpansionVessel} = 20 \frac{W}{m^2} A_{SF} \frac{T_{avg}}{343°c} + 2.57 MW_{th} \frac{T_{avg}}{275°c} \quad (5)$$

Where, A_{SF} : the collector aperture area; T_{avg} : the mean solar field temperature.

3.4. Trough solar system design conditions:

This paper uses the meteorological data of the typical year in Chinese Yinchuan from the TRNSYS meteorological database, the average daily changes of solar radiation over time for each quarter are shown in Fig. 2. Table 5 lists the respective design data for each quarter. This paper maintains the minimum temperature difference about 8℃ between the conductive oil and water in the heat exchanger, in order to compare the performances of different integration schemes.

Table 5. Solar design values of each quarter

Time (hr)	(0-8760)	Zenith	Azimuth	Wind speed	Ambient temperature	DNI(kJ/hr. m^2)
First quarter	1885.5	39.5°	4.68°	2.350 m/s	9.4℃	3217.39
Second quarter	3637	16.6°	-6.27°	3.100 m/s	24.1℃	3920
Third quarter	4405.5	15.9°	13.5°	2.430 m/s	30.2℃	3756.39
Fourth quarter	6610.5	55.3°	-47.1°	0.725 m/s	10.5℃	1474.14

4. The simulation results

The thermal energy incoming ($Q_{EnergyIncoming}$) of every integration position of the combined cycle has a maximum heat load limit ($Q_{MaximumHeatLoad}$), the heat transfer process of fuel gas and water in HRSG will violate the law of heat transfer if the energy incoming exceeds the maximum heat load limit. The design factor (*DF*) is proposed to measure the scale of integrated solar energy. It is defined as the ratio of the $Q_{EnergyIncoming}$ from the solar energy system with the design data to the $Q_{MaximumHeatLoad}$ of integration position of combined cycle system. The calculation formula of *DF* is as follows:

$$DF = \left(Q_{EnergyIncoming}\right) \Big/ \left(Q_{MaximumHeatLoad}\right) \tag{6}$$

The annual thermal efficiency η of the solar energy side is defined a ratio of the increased power output of ISCC system relative to the GTCC system to the received solar energy (Q_{solar}) of trough solar system during one year. The quarterly thermal efficiency of the solar energy side has a similar definition. The formula is as follows:

$$\eta = \left(W_{ISCC} - W_{GTCC}\right) \Big/ Q_{solar} \tag{7}$$

Where, W_{ISCC}: the power output of ISCC system; W_{GTCC}: the power output of GTCC system.

The day prolific power is a parameter that averages the entire annual prolific power of solar energy into a day.

4.1. The integration characteristics of single section

The monotonically increasing process of the annual thermal efficiency with the increase of the integrated solar collector aperture area is shown in Fig. 3, with the increase of the integrated solar collector surface area, the heat loss per power is reduced and the exhaust gas temperature of HRSG is also reduced, which realized the better use of the thermal energy of gas turbine exhaust gas, therefore the solar system shows better thermodynamic performances. The rightmost point of every curve is designed in *DF*=1 and the detailed data are shown in Table 6. As shown in the Fig. 3, the

LPB integration is the optimal in the area ranges of 5000m^2 to 17000m^2 and 8700m^2 to 10210m^2, the LPS integration is the optimal in the area range of 8700m^2 to 9666m^2. Within the area range of 17000m^2 to 111158m^2, the IPB integration has the maximum annual efficiency, the day prolific power is 66903kW·h (*DF*=1) more than 66604kW·h when HPB integration is designed in *DF*=1. The dotted oblique equipower line is drew by integrated performance of integrated system, compared with LPB integration, the IPB integration can save about 39842m^2 area under the same the day prolific power. Although the higher integrated temperature is good for the Rankine cycle performance improvement, however, in the limited integrated area, with the increase of the average integrated temperature, the thermal efficiency of collector reduces and the total heat loss increases, so the IPB integration has better performance than the HPB integration.

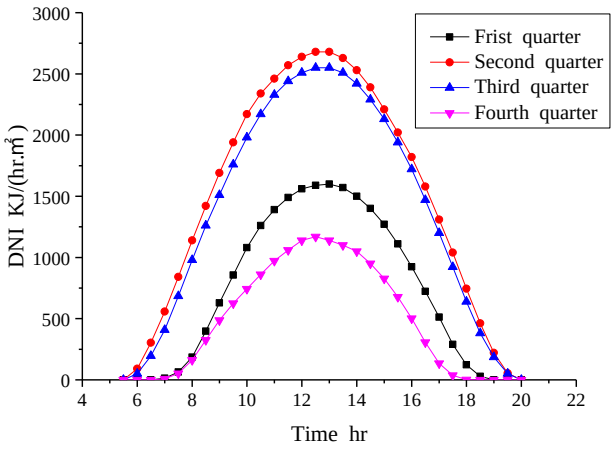

Fig. 2 Average solar radiation of each quarters

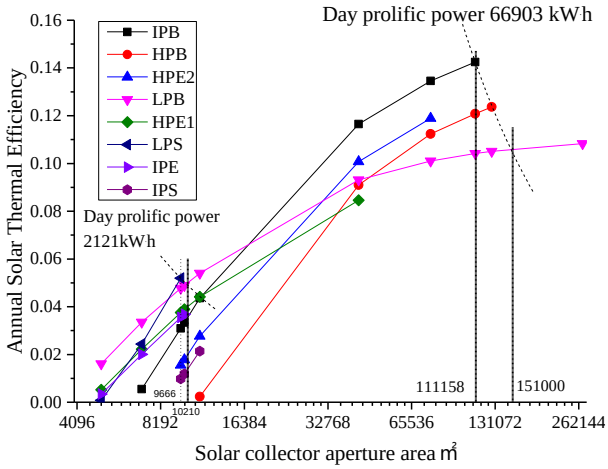

Fig. 3 The annual solar thermal efficiency varies with the integrated area

Table 6. Simulated data in design data of second quarter

Aperture area(m^2)	Position	DF	Power	Efficiency	Aperture area(m^2)	Position	DF	Power	Efficiency
270824	LPB	1	40.2MW	0.1084	11328	IPS	1	1.6MW	0.0214
9666	LPS	1	1.7MW	0.0519	42311	HPE1	1	5.8MW	0.0846
9962	IPE	1	1.1MW	0.0369	76796	HPE2	1	17.4MW	0.1190
111158	IPB	1	26.6MW	0.1425	127428	HPB	1	35.1MW	0.1237

4.2. The simultaneous integration characteristics of two sections

The simulated data of simultaneous integrations of two sections show that the day prolific power is the sum of integrated power alone. When the total integrated solar collector aperture area is constant, the solar annual efficiency of simultaneous integrations of two sections is shown in equation:

$$\eta_3 = \left(\eta_1 \cdot A_1 + \eta_2 \cdot A_2\right) / \left(A_1 + A_2\right) \tag{8}$$

Where, η_n: the solar annual efficiency of section n; A_n: the integrated solar collector aperture area of section n; η_3: the solar annual efficiency of simultaneous of two sections with aperture area of A_1+A_2.

Equation (8) shows that the efficiency of simultaneous integrations of two sections is between the minimum and maximum efficiency of each single-integration. So within the area range of 5000m^2

to 111158m^2, the optimal integration scheme is shown in Fig. 3. This paper focuses on the integration that IPB combines with any other section and identifies the optimal integration scheme in the limited integrated area. The simulated data of simultaneous integrations of two sections show that there is mutual restraint of the largest integrated scale of two sections. Such as when the IPB section is designed in *DF*=1, the maximum design *DF* values of HPE2, LPS, HPB and LPB sections are 0, 0, 0.6452 and 0.6167, respectively. Fig. 4 shows the day prolific power under the largest area combinations of IPB with HPE2 and LPB, with the increase of IPB integrated area, the largest integrated areas of HPE2 and LPS are restricted by the law of heat transfer. The largest integrated area of combination of IPB and HPE2 can be greater than 111158m^2, and the largest integrated area of combination of IPB and LPS is less than 111158m^2. Because the largest day prolific power occurs in the situation when the *DF* of IPB is 1, in the limited area (more than 111158m^2), these two simultaneous integrations are not the optimal integration scheme.

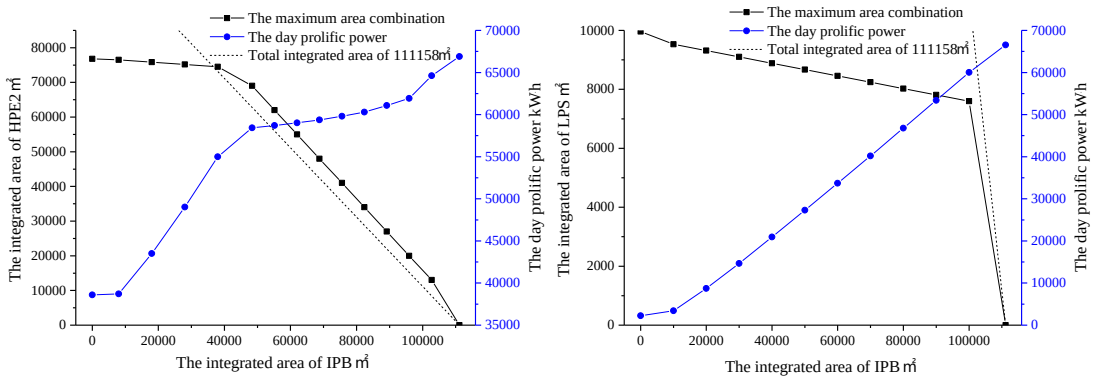

(a) *(b)*

Fig. 4 The day prolific power under the maximum area combination: a) IPB and HPE2, b) IPB and LPS.

Fig. 3 shows that the annual efficiencies of LPB and HPB respectively are the highest in the limited integrated solar aperture area except for the IPB, HPE2 and LPS, so the optimal simultaneous integration occurs in the situation when the IPB combines with LPB or HPB. Fig.5 shows the annual solar thermal efficiency curve under the different integrations of IPB with LPB and HPB. In the simultaneous integration of IPB (*DF*=1) with LPB, the annual efficiency is the highest in any limited area, and there is the largest combinational design output power of 52.6MW with the integrated area of 287008m^2. In the simultaneous integration of IPB (*DF*=1) with HPB, the annual efficiency is the highest in any limited area, and there is the largest combinational design power of 49.2MW with the integrated area of 195517m^2. The reason can be explained with the mathematical relationship (8).

The simultaneous integrations of IPB (*DF*=1) with any other section are shown in Fig. 6. Under the total integrated area of 127428m^2 (*DF* of HPB is 1), the maximum simultaneous integration efficiency is 13.29%, 0.92% more than 12.37% (the integration efficiency of the single HPB). When the total integrated area is 270824m^2 (*DF* of LPB is 1), the maximum simultaneous integration efficiency is 12.12%, 1.28% more than 10.84% (the integration efficiency of the single LPB). In Fig. 6, the rightmost point corresponds to the integrated area of 287008m^2, the annual solar thermal efficiency of 12.06% is higher than the efficiency (11.90%) of HPE2 when *DF*=1. So in the integrated area range of 111158m^2 to 287008m^2, the optimal simultaneous integration of any two sections is shown in Fig. 6. The intersection of HPB line and LPB line is the corresponding integrated area of 156158m^2. When the total integrated area is 195517m^2, the simultaneous

integration efficiency of IPB and HPB is 13.05% and the day prolific power is 10779.5kW.h, under the same day prolific power, that can save about the integrated area of 9641m^2 for the simultaneous integration of IPB and LPB. So the simultaneous integration of IPB (*DF*=1) and LPB is the optimal in the total area ranges of 111158m^2 to 156158m^2 and 205158m^2 to 287008m^2, the simultaneous integration of IPB(*DF*=1) and HPB is the optimal in the total area range of 156158m^2 to 195517m^2.

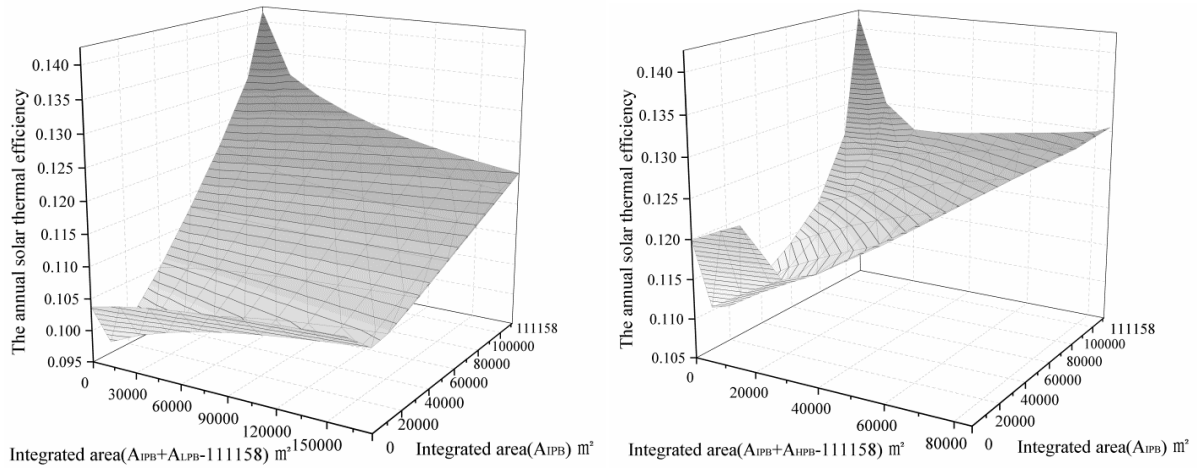

(a) *(b)*

Fig. 5 The annual solar thermal efficiency under the simultaneous integration : a) IPB and LPB, b) IPB and HPB.

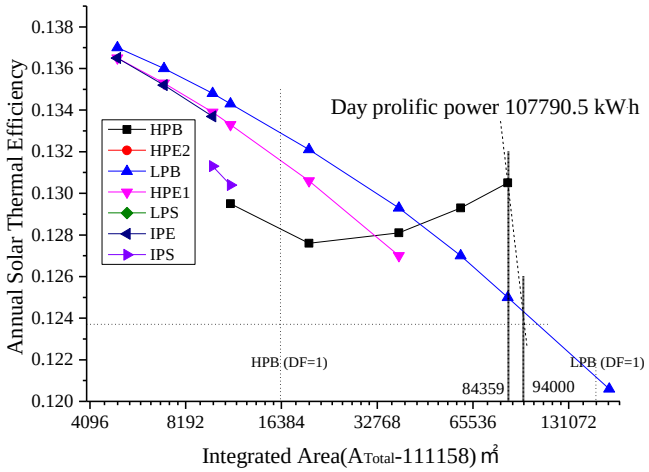

Fig. 6 The annual solar thermal efficiency under the IPB(DF=1) simultaneous integration with other sections

4.3. The performance comparison with the independent solar thermal power generation without integration with GTCC

Since 1985-1991, America has already commercially operated some trough solar thermal power plants. Their performances are listed in Table 7 which shows that the system thermal efficiency increases with the increase of the system power. With the improvement accumulations of technology and the accumulations of operational experience, the annual solar thermal efficiency of 30MW power plants has increased from 10.7% to 12.4%. Based on the above research results in this paper, when IPB section of HRSG is integrated with the solar energy and *DF* is 1, the design

power of solar energy side is 26.6MW and the annual solar thermal efficiency is 14.25% (see *Table 5*). In the optimal integration scheme of this paper, the maximum annual solar thermal efficiency is 13.2% when the design power is 30MW (the integrated area 24878m^2 in *Fig.6*). It can be seen, the integrated solar combined cycle power generation is not only an effective solution to overcome solar radiation fluctuation and some technology bottlenecks which include the immature heat storage technology, but also it has a relatively obvious advantage in transferring the solar energy to power.

4.4. The quarterly integration characteristics of the single section

The variation rules of the quarterly solar energy thermal efficiency with the integrated area, with the single section integration, are shown in Fig. 7, the rightmost point of every curve is the largest integrated scale in each quarter. When the solar radiation is not rich (first and fourth quarter), the integration of low temperature (integration of LPB) has a relative advantage, the integration of the high temperature section (integration of HPB) is not proper, because the thermal efficiency of the collector decreases and the total heat losses of the trough solar system increases with the increase of the integrated temperature. According to the integrated characteristic of each section in each quarter, the operational temperature and integrated position of HRSG will be changed to gain more power in the limited integrated aperture area. For example, when the integrated IPB section is designed with the *DF* of 1 (the integrated area is 111158m^2), its design power is 26.6MW and the annual efficiency is 14.25%, integrating with LPB section in the first and fourth quarters and IPB section in the second and third quarters, in the limited aperture area of 111158m^2, its efficiency is 14.61%, 0.36% more than the original efficiency of 14.25%. When the design power is 30MW, the optimal integration in this paper is that IPB (DF=1) combines with LPB (the total integrated area is 136036m^2), integrating with LPB section in the first and fourth quarters, the original integration is unchanged in the second and third quarters, in the limited aperture area of 136036m^2, its annual efficiency is 14.29%, 1.09% more than the original efficiency of 13.2% and 1.89% more than the maximum efficiency of 12.4% in 30MW SEGS plants. So based on the quarterly integration nature, the reasonable quarterly integration can have a better operation performance.

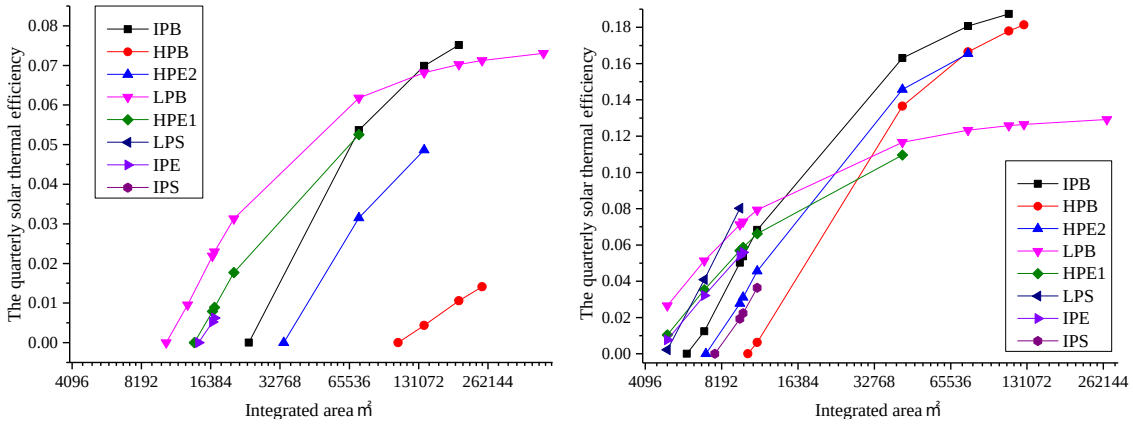

(a) *(b)*

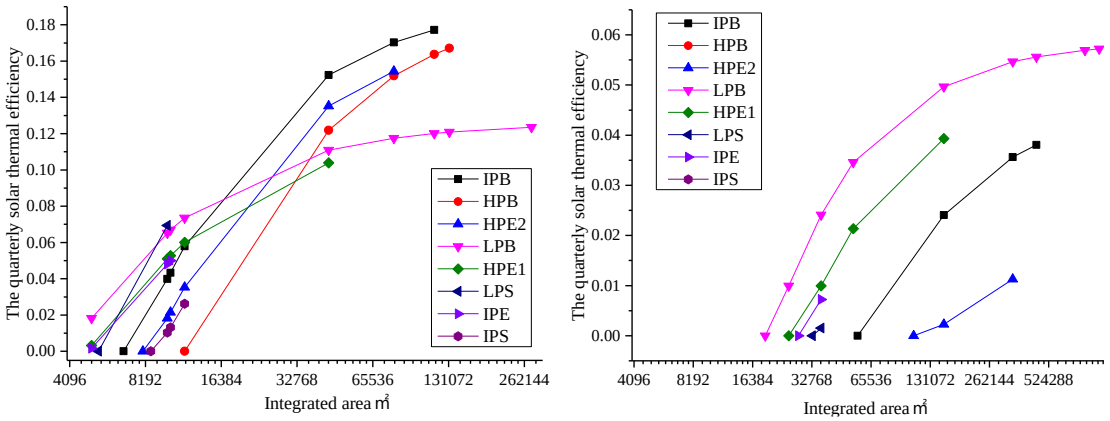

(c) *(d)*

Fig. 7 The quarterly solar thermal efficiency varies w he integrated area in different quarters: a) first quarter, b) second quarter, c) third quarter, d) fourth quarter.

Table 7. Data of the SEGS parabolic trough solar power plants in California, USA

Plant name	SEGS I plant	SEGS II-VII plants	SEGS VIII and IX plants
Number of plants	1	6	2
Start year of operation	1985	1986-1989	1990-1991
Power(MW)	14	30	80
Max fluid temperature(°C)	307	350 and 390	390
Annual average efficiency (%)	9.3	10.7-12.4	13.8

5. Conclusion

On the base of a gas steam combined cycle system (GTCC) with a three-pressure reheat recovery steam generator (HRSG), an integrated trough solar energy combined cycle system (ISCC) without thermal energy storage is designed. The optimal integrated schemes of ISCC in the limited aperture area are deeply investigated, including the single section integration, the simultaneous integration of two sections and quarterly integration of single section. The research results show the annual solar thermal efficiency increases with the increase of design power in the different integrations. When two sections of HRSG simultaneously integrate with the solar system, the total integrated solar energy output power is the algebra of integrated power alone. When the design power is 30MW, in this paper, the maximum annual solar thermal efficiency is 13.2%, 0.8% more than the maximum efficiency of 12.4% in 30MW California solar energy generating systems SEGS plants. According to the quarterly integration characteristics of single section, the reasonably selecting the integration temperature and position in each quarter is necessary to improve the gain of the solar energy power generation at the hybrid solar/fossil operation.

Acknowledgments

This study has been supported by the National Nature Science Foundation Project (No.51276063) and the National Basic Research Program of China (No.2015CB251505).

References

Web references:

[1] Electric Power Research Institute. Solar Thermal Electric Technology: 2006 – Available at:< http://www.epri.com/search/Pages/results.aspx?k=Solar%20Thermal%20Electric%20Technology%3A%202006>[accessed 30.3.2007].

[2] China National Renewable Energy Center. China Wind, Solar and Bioenergy Roadmap 2050 Short Version – Available at:< http://www.cnrec.org.cn/cbw/zh/2014-12-25-456.html>[accessed 25.12.2014].

[3] International Energy Agency. Technology Roadmap: Solar Thermal Electricity - 2014 edition – Available at:<http://www.iea.org/publications/freepublications/publication/technology-roadmap-solar-thermal-electricity---2014-edition.html>[accessed 9.2014].

Journals:

[4] Haixiang Zang, Qingshan Xu, Haihong Bian, Generation of typical solar radiation data for different climates of China. Energy 2012;38:236-248.

[5] D.Mills, Advances in solar thermal electricity technology. Solar Energy 2004;76:19–31.

[6] Giovanna Barigozzi, Giuseppe Franchini, Antonio Perdichizzi, Silvia Ravelli, Simulation of Solarized Combined Cycles :Comparison Between Hybrid Gas Turbine and ISCC Plants. Journal of Engineering for Gas Turbines and Power 2014;136:1-10.

[7] G. Franchini, A. Perdichizzi, S. Ravelli, G. Barigozzi, A comparative study between parabolic trough and solar tower technologies in Solar Rankine Cycle and Integrated Solar Combined Cycle plants. Solar Energy 2013;98:302-314.

[8] A. Baghernejad, M. Yaghoubi, Exergoeconomic analysis and optimization of Integrated Solar Combined Cycle System (ISCCS) using genetic algorithm. Energy Conversion and Management 2011;52:2193-2203.

[9] A. Baghernejad, M. Yaghoubi, Exergy analysis of an integrated solar combined cycle system. Renewable Energy 2010;35:2157-2164.

[10] G.C.Bakos, D.Parsa, Technoeconomic assessment of an integrated solar combined cycle power plant in Greece using line-focus parabolic trough collectors. Renewable Energy 2013;60:598-603.

[11] M.J.Montes, A.Rovira, M. Muñoz, J.M. Martínez-Val, Performance analysis of an Integrated Solar Combined Cycle using Direct Steam Generation in parabolic trough collectors. Applied Energy 2011;88:3228-3238.

[12] Antonio Rovira, María José Montes, Fernando Varela, Mónica Gil, Comparison of Heat Transfer Fluid and Direct Steam Generation technologies for Integrated Solar Combined Cycles. Applied Thermal Engineering 2013;52:264-274.

[13] Guillermo Ordorica-Garcia, Alfonso Vidal Delgado, Aranzazu Fernandez Garcia, Novel integration options of concentrating solar thermal technology with fossil-fuelled and CO2 capture processes. Energy Procedia 2011;4:809-816.

[14] J. B. Young, R. C. Wilcock, Modeling the Air-Cooled GasTurbine: Part 1—General Thermodynamics. Journal of Turbomachinery 2002;124:207-213.

[15] J. B. Young, R. C. Wilcock, Modeling the Air-Cooled GasTurbine: Part 2—Coolant Flows and Losses. Journal of Turbomachinery 2002;124:214-221.

[16] R. C. Wilcock, J. B. Young, J. H. Horlock, The Effect of Turbine BladeCooling on the Cycle Efficiency ofGas Turbine Power Cycles, Journal of Engineering for Gas Turbines and Power 2005;127:109-120.